The Decay of Space Charge in a Glassy Epoxy Resin following Voltage Removal

L.A.Dissado[1], V.Griseri[1,2], W.Peasgood[1,3], E.S.Cooper[1], K.Fukunaga[4], J.C.Fothergill[1]

1. Department of Engineering, The University of Leicester, Leicester U.K.
2. Now at Lab.Genie Electrique, University Paul Sabatier, Toulouse France
3. Now at Clinical Physics and Bioengineering Radiotherapy Centre, Walsgrave Hospital, Coventry, U.K
4. EMC group, Communication Research Laboratory, 4-21, Nukui-Kita, Konagei, Tokyo, Japan

ABSTRACT

The PEA technique is used to measure the distribution of space charge in an epoxy resin after polarisation for one week at an applied field of 7.14kV/mm over a range of temperatures. The decay of the space charge is followed for times up to 114 hours after removal of the voltage and analysed in terms of a number of alternative decay mechanisms. It is shown that the rate-determining stage of the decay mechanism is that of a thermally activated process that has been associated with charge de-trapping. At times greater than 10^2s the de-trapping process behaves as though the space charge field does not exist and the retention time of the space charge depends only upon the depth of the deepest occupied traps and the temperature.

Keywords: Space Charge, De-trapping, Epoxy Resin

1. INTRODUCTION

The generation of space charge in insulators under voltage alters the field distribution from that that would apply in its absence. Local fields can be produced that are more than double the average applied field (for example see [1, 2]). Consequently space charge evolution can represent a potential threat to the integrity of insulating materials under electric stress [1, 3]. A further problem in insulation design is posed by the retention of space charge in traps after the applied voltage has been removed (for example see [2]). This results in long-lived currents following short-circuit, and also in severe field modification during polarity reversal, in DC conditions. It may also lead to charge accumulation from one ½-cycle to the next in AC conditions [4]. The aim here is to investigate the mechanism whereby space charge decays in an epoxy resin in its glassy state, in order to elucidate the decay mechanism and determine the material factors that control its rate. An analysis of this type may potentially establish guidelines for the assessment of the quality of different insulation materials and allow changes in insulation quality caused by ageing to be quantified.

The various possible origins for the space charge measured in insulating polymers mean that it is unlikely that a general description of its decay can be formulated. For example, space charge injected from an electrode may decay following voltage removal by a number of routes; i.e. de-trapping and extraction at the injecting electrode; transit of the sample and extraction at the counter-electrode: or injection of neutralising charge of the opposite polarity. Space charge generated by ionisation of entities with donor or acceptor states may decay by transit of the mobile carrier and recombination or by neutralisation via injected charge of opposite polarity. However, space charge generated by ionisation to form molecular ions is likely to decay by transit and recombination. Neutralisation by charge injection from the electrodes may either be impossible because the neutral species may be non-existent, or could lead to damaging electrolytic reactions.

Examples of some of these processes may be found already in the literature. In [5] simultaneous measurement of space charge by the thermal pulse method and the external current showed that the decay of space charge in an anti-static doped high-density polyethylene (HDPE) following short-circuit was governed by the injection of negative charge. This injection neutralised positive heterocharge (charge of opposite polarity to the electrode) that had formed next to the cathode. The positive heterocharge was associated with the anti-static agent, and most probably was produced in the form of ionised donor molecules. The injection current was demonstrated to have the Schottky form (e.g. [6]),

$$I_{inj} = I_o exp(-\phi/kT)exp\{e(eE_e/4\pi\varepsilon_o\varepsilon_r)^{1/2}/kT\} \qquad (1)$$

Here E_e is the electrode field, ϕ is the energy barrier for charge injection, and ε_r is the relative permittivity of the dielectric material. In thick (1 to 2mm) films [7] of low-density polyethylene (LDPE) the decay of the space charge was mainly due to charge transit and recombination although close to the electrode charge injection also played a role. This was particularly the case at T = 70 °C where, as with HDPE, the charges were mainly hetero-charge, and the injection current followed the Schottky law. In both these cases therefore Schottky injection plays a role in the decay of the space

charge even though the electrode material was very different, i.e. gold in the HDPE case, and carbon loaded polymer (C-black semicon) in the LDPE case.

Thermally stimulated depolarisation currents (TSDC) [8] show that charge in insulators is trapped at a range of trap depths. It would therefore be expected that transit and recombination or neutralisation at the electrode would be governed by de-trapping. The experiments reported in [7] could not distinguish between a transport mechanism controlled by field-assisted thermally activated hopping between neutral sites or a Poole-Frenkel process [6]. It was shown in [9] however, that the decay of space charge in an epoxy resin was controlled by the time dependent de-trapping of the injected charge from trap sites whose trap depths uniformly covered a range of energies. In this case a geometrically divergent field was investigated and therefore it could be expected that on de-trapping the main part of the injected charge would move rapidly to the neighbouring injecting electrode for extraction, rather than travel to the planar counter-electrode. The assumption that space charge decay was governed by the transport of charges to the electrodes for neutralisation has recently been used to derive an approximate expression allowing the time dependent mobility of such charges during the decay process to be extracted from the time dependent space charge magnitude [10, 11]. The results for cross-linked polyethylene (XLPE) imply an effective mobility governed by trap-to-trap hopping between ever deeper traps as the remaining space charge density decreases.

This investigation concentrates upon space charge decay in thin films of an epoxy resin. Epoxy resins provide a substantial contrast to the polyethylene class of insulator in that instead of being semi-crystalline their morphology has the form of a 3D-network. In addition their chemical composition is very different. Consequently they could be expected to possess a greater trap density than polyethylene and their traps are likely to range to deeper energies. Unlike the situation discussed in [9], a parallel-plate electrode geometry has been used. In this way we reduce the likelihood of traps generated near the electrodes by the sample manufacturing procedure. The resin is primarily investigated when in its glassy state so that a comparison can be made with the rubbery polyethylenes investigated in [5, 7]. Some measurements have also been carried out above the glass transition temperature in order to separate the effect of morphology from that of chemistry. Rather than assume that space charge decay is determined by transit to a neutralising electrode a number of decay mechanisms will be evaluated for their ability to fit the observed change of space charge density. This approach is intended to provide a means of analysing data in order to both identify the decay mechanism and to extract pertinent parameter values.

2. EXPERIMENTAL

2.1 Material and Measuring System

The epoxy resin used was prepared from the mixture of the Araldite base resin CY1301 and the hardener HY1300. The base resin is essentially composed by Diglycidyl Ether-Bisphenol A (DGEBA) and Iso-Octyl Glycidyl Ether (IOGE) whereas the hardener is a mixture of Triethylene Tetra Amine (TETA) and Polyoxypropylene as major components. The samples were produced in the form of thin films with a thickness varying between 250 and 300 μm. When placed under DC voltage space charge developed in the samples and this was measured using a pulsed

electro-acoustic (PEA) system [12]. In the measurements the lower electrode was aluminium while the upper electrode through which the high voltage was applied was a carbon black loaded conducting polymer, which in some cases was covered with a conducting layer of aluminium. The probe pulse used in the experiments had a pulse width of 5ns, a repetition frequency of 400Hz, and amplitude of 400V.

The glass transition temperature of the epoxy was determined by Differential Scanning Calorimetry (DSC) technique to be about 40°C. All experiments reported here were carried out at controlled temperatures above and below the glass transition.

2.2 Experimental protocol

Two sets of experiment were carried out. In the first set a DC voltage of +2kV (electric field = 7.14 kV/mm) was applied to the samples via the top electrode for a time of one week at T = 25 °C. The results reported here relate to the decay of the space charge over a period of 68h following the removal of the voltage. In the second set of experiments the same DC voltage of +2kV (E = 7.4kV/mm) was also applied for 1 week, but the decay was followed over a longer period of time and at different temperatures, namely 101 h at T = 20 °C, and 114 h at T = 33°C. In addition some experiments were carried out at 50 °C, i.e. above the glass transition, with a DC voltage of +2KV (electric field = 6.7kV/mm).

3. SPACE CHARGE MEASUREMENTS

3.1 Homocharge Peaks

In measurements made under voltage the signal from the electrodes are too strong to reveal the bulk space charge with any accuracy. The main indication of its presence is a small displacement of the signal from the electrode into the sample that implies the presence of injected charge of the same polarity as the electrode, termed homocharge. The signal displaces because the homocharge induces a charge on the electrode of opposite polarity while it builds up trapped charge of the electrode polarity in the bulk. The existence of such homocharge is demonstrated conclusively by the signal obtained when the voltage has been removed. These signals show that a positive homocharge peak has developed in the epoxy resin over the time under electrical stress see figure 1. These results are qualitatively the same as those found previously at much higher applied fields (18kV/mm to 180kV/mm) [13]. It seems clear from the position of the peaks and the measurements made during voltage application that the injected charge did not move very far into the epoxy film before being trapped. Because of attenuation and dispersion of the acoustic wave during transit of the sample the estimated magnitude of the space charge near the upper electrode is less accurate than that closer to the piezo-electric detector located beneath the lower electrode. For this reason we will concentrate our analysis of the space charge decay upon the homocharge peak next to the lower electrode.

3.2 Apparently long-lived Electrode Peaks

A curious feature of this data is that 48 hours after the removal of the applied voltage the peak on the electrode becomes zero leaving only one peak in the charge density occupying the position of the homocharge peak close to the bottom electrode.

Furthermore, as shown in figure 1, this peak hardly seems to decay at all over the subsequent 20 hours (i.e. between 48 and 68 hours after the voltage has been removed). Although it was impossible to resolve a homocharge peak near the upper electrode the broad peak there also showed very little decay over the period of 48-68 hours after voltage removal. A similar behaviour was found in all the other experiments that have been performed, although the time at which it occurred varied depending upon the temperature. The expected behaviour when bulk space charge is present, as here, is that it will induce an image charge on the electrode that will yield a signal of opposite sign proportional in magnitude to the bulk space charge density. It is shown in figure 2a that this is the case for the period of time when two peaks can be observed in the PEA signal. The extrapolation to zero electrode charge corresponds to the observed peak magnitude at the position of the homocharge peak, which is retained beyond the time scale of the experiment.

In [14] and [15] it was shown that the signals proportional to the probe perturbation (V_p) gave the same information about the electrical state of a sample in both the PEA and Laser Induced Pressure Pulse (LIPP) techniques (see equations (38) and (36) of [14] and equations (23) and (10) of [15]). This is expressed through a contribution to the signal proportional to the gradient in electric field due to bulk space charge and electrode charge (see equation (38) of [14]). It is this first order (linear) response to the probe perturbation that is usually used to interpret and predict the signals (see for example [16]). However, it was pointed out in [14] and [15] that a second order contribution that is proportional to the square of the probe perturbation (i.e. $(V_p)^2$) also exists, but that where the probe perturbation is a pressure wave (as in LIPP) this second order contribution is negligible compared to that of the first order. On the other hand this is not always the case for the PEA measurement, as for example in a geometrically divergent field [17]. In the case of parallel plate geometry it was shown that the contribution of the second order term was restricted to a signal from the electrode interfaces (see equation (23) of [15]). These contributions will be a significant part of the total electrode signal when the field due to the probe pulse voltage is not negligible with respect to the total electrode field from the space charge and applied voltage. Such a situation is unlikely to arise during the period of voltage application, but will probably occur at some stage after the removal of the applied voltage when the space charge field becomes low. Unlike the first order signal the magnitude of the second order signals will be independent of the polarity of the probe pulse. They will also have opposite signs at each interface [15].

The second order signals are effectively self-generated responses to the probe and can be measured before the application of a potential to the sample. Figure 2b, shows such a measurement made at T = 20 °C. It was suggested in [14] that their influence be removed by subtracting signals made with a negative probe voltage from those made by a positive probe voltage. This is not easy to carry out with our system and since the contribution is small in comparison with the signals obtained on removal of the applied voltage such a procedure was not carried through. However, it can be seen that the amplitude of the second order contribution is close to that of the space charge measured when the electrode peak disappears, see figure 2a. This leads to two alternative explanations for the single peak observed near the lower electrode at long times: either there is no space charge present and the peaks measured are solely due to the second order term, or that the second order term has cancelled the signal due to

the image charge on the electrodes leaving only the first order signal due to the space charge to be measured.

In order to investigate the situation a series of experiments were performed after 114 hours decay at 33°C. The results are shown in figure 3. Figure 3a demonstrates the procedure adopted to produce the traces shown in figure 3b. Initially (trace 1) only two peaks were observed one near each electrode. We then reversed the sample in the measuring system, and found that the peak at the upper electrode almost disappeared whereas two peaks of opposite polarity were found at the lower electrode (trace 2). This measurement reveals the presence of negative space charge in the sample on the side that was originally near the upper electrode. The first and second order contributions to the lower electrode signal are both positive and reinforce one another. The signal from the upper electrode in trace 2 indicates a near cancellation of the positive space charge now located there and the net of the first and second order electrode contributions, which will both be negative. The polarity of the probe pulse was now reversed keeping the sample in the same orientation. This will alter the sign of the first order (linear) contribution and hence of the space charge signals, but will not affect the polarity of the second order contribution. The measurements (trace 3) now show just one positive polarity peak at the lower electrode and a negative polarity peak on the upper electrode. The behaviour at the lower electrode implies that the first and second order contributions from the electrode nearly cancel leaving only the space charge signal, which is now positive because of the change in polarity of the probe pulse. The appearance of a peak of opposite sign near the upper electrode in this configuration shows that there is space charge in the sample on this side also. Because of the reversal of the probe pulse the signal from this charge will now be negative and is reinforced by a net electrode signal, which is negative. In order to reveal this more clearly the sample was returned to original orientation, while retaining the keeping sign of the probe pulse the same as that in trace 3, i.e. still opposite to its original polarity in trace 1. The results, given in trace 4, show a double peak at the lower electrode and essentially no peak at the upper electrode, thereby verifying the existence of space charge near the bottom electrode in the original orientation. Again the space charge signal from the side near the top electrode was essentially cancelled by negative net signal from the electrode. Trace 5 shows the behaviour when the probe pulse polarity was returned to that of trace 1. These experiments show that the presence of just two peaks in the signal a long time after the voltage has been removed does not mean an absence of space charge but rather that the second order contribution from the electrodes has a major effect upon the electrode signal. In our case space charge has been shown to be present on both sides of the sample even more than 100 h after the voltage has been removed.

4. SPACE CHARGE DECAY

The results discussed in section 3 shows the existence of homocharge peaks near to the electrodes. Ionic dissociation of any kind or injection and charge transit would give rise to heterocharge. These peaks must therefore be due to charge injection followed by trapping. In principle the PEA technique could detect 'free charge' since the force terms in equation (1) do not distinguish between free and trapped charge. The finite duration of the probe pulse ($\sim$ 5ns) however, allows time for 'free charge' to displace during its application. As a result the compressive (rarefaction) waves (see

[18]) that travel towards the detector are cancelled by compensating rarefaction (compressive) waves produced earlier in the pulse and moving in the opposite direction. We must therefore consider the homo space charge to be trapped.

4.1 Charge De-Trapping

A number of possible mechanisms for space charge decay may be active in our experiments. Charge may be de-trapped and move to a neighbouring electrode for extraction. Charge may be de-trapped and transit the sample for neutralisation by space charge of opposite polarity. Neutralising charges may be injected from the neighbouring electrode. There are three basic mechanisms involved in these processes, charge de-trapping, charge transport, and charge injection. Each of these mechanisms may have different timescales of operation.

In [9] it was shown that space charge decay in an epoxy resin could be described very well by the assumption that the rate-determining step is an isothermal de-trapping process, which released charge for neutralisation at an adjoining wire electrode. In actuality the transport of the charge to the extracting electrode would involve multiple trapping and de-trapping processes, however it has been shown [19] that the single de-trapping approximation gives very good estimations of the energy distribution of the trapping states lacking only details of the fine structure. These results indicate that for the thin films considered, multiple trapping and de-trapping is dominated by just a single de-trapping event from a trap whose energy lies at the top of the filled range, i.e. the deepest trap state available for trapping.

In principle the analysis described in this sub-section applies equally to de-trapped charges that transit the sample for neutralisation by opposite polarity homo-charge as to charges that move to a neighbouring electrode to be neutralised. However, the sample is much thicker than those considered in [19] and in this case it can be expected that multiple trapping will result in many de-trapping events from states at the top of the filled energy range. This will result in a time scale for transit and decay whose activation energy will be the same as for the single trapping analysis, but for which the effective attempt frequency will be much lower, since the transit time (and mobility) will also be determined by the number of de-trapping events.

 In our experiments the field between the two space charge peaks is small once the voltage is removed whereas that between a peak and its neighbouring electrode is large. Therefore most of the injected charge can be expected to move towards the neighbouring electrode for neutralisation rather than transit the sample, a short enough distance for the single de-trapping approach to give an adequate description. In support of this contention there is no evidence for a broadening of the space charge peaks, such as would be expected if a substantial portion of the space charge were to move across the sample via a sequence of multiple trappings and de-trappings.

If the traps are taken to have a constant density in trap depth and to be filled from a maximum trap depth Δ_{max} up to a trap depth of Δ_{min}, the time dependence obtained for space charge density is given by following equations,

$$\rho(t) = \rho(0) \qquad t < [\nu \exp(-\Delta_{min}/kT)]^{-1} \tag{2}$$

$$\rho(t) \approx [\rho(0)kT/(\Delta_{max} - \Delta_{min})](a - \ln(t)) \qquad [\nu\exp(-\Delta_{min}/kT)]^{-1} < t < [\nu\exp(-\Delta_{max}/kT)]^{-1}$$
$$\tag{3}$$

$$\rho(t) = 0 \qquad [\nu\exp(-\Delta_{max}/kT)]^{-1} < t \tag{4}$$

In this set of equations ν is the attempt to escape frequency, $\rho(t)$ is the time-dependent space charge density, and a is a factor (with units of ln{frequency}) that is independent of time. The derivation [9] is given in Appendix 1. This behaviour can be revealed by plotting $\rho(t)$ as a function of log(t), in which format a sigmoidal form is obtained, see figure 3 of [9]. Essentially it can be interpreted to mean that very little decay occurs until the time, t_1,

$$t_1 = [\nu\exp(-\Delta_{min}/kT)]^{-1} \tag{5}$$

at which the shallowest occupied traps (Δ_{min}) start to be emptied. Then the logarithmic dependence sets in while the traps are emptied from the top down, [19]. This phase of the decay ends when the deepest traps (Δ_{max}) start to be emptied at t_2,

$$t_2 = [\nu\exp(-\Delta_{max}/kT)]^{-1} \tag{6}$$

If the energy distribution of the traps is not constant, but contains peaks [7] we can expect a form similar to equation (3) but with steps in the linear feature of the $\rho(t)$ vs log(t) plot.

Plots of $\rho(t)$ as a function of log(t) constructed from data at T=20°C, T=25°C, and T=33°C are given in figure 4. A region of near constant $\rho(t)$ is found between 10^2s and 10^3s, followed by a linear dependence of $\rho(t)$ upon -log(t) as predicted by equations (2) and (3). It is therefore a reasonable assumption that the single de-trapping theory holds for $t \geq 10^2$s. Δ_{min} can be estimated by taking t_1 as the time where the proportionality of $\rho(t)$ to ln(t) sets in and assuming that $\nu = kT/h$.. Taking the magnitude of $\rho(t)$ at the times 10^2 s to 10^3 s to be the value of $\rho(0)$ for the charge de-trapped from the trap distribution described above, a value for Δ_{max} can be estimated from the gradient in the region where equation (3) holds. These estimates are used in the exact expressions (equation (25) in Appendix 1) to give the theoretical single de-trapping space charge decay curves that best fit the data, shown as the lines in the plots of figure 4. The best fit values of Δ_{min} and Δ_{max} are given in Table 1. The estimated values of Δ_{max} lie between 1.1 and 1.14eV and are sufficiently large that the release time of charge from the deepest traps is in excess of the longest time of the experiment (~ 100 h). This implies that some trapped charge is still present at the end of the experiment, as shown in figure 3.

The theoretical curve fits the data at T=25°C over the whole measurement time range, but data obtained at T=20°C and T=33°C show an upwards deviation from the theoretical curve at short times ($t < 10^2$s) where there are no measurements at T=25°C. There are a number of possible explanations for this deviation. In the first place there may be a distribution of shallower traps that release their charge on a shorter timescale. In the absence of measurements at shorter times this cannot be ruled out as a possible explanation. If such a trap distribution exists the most that can be deduced about it from the limited data available is that the energy of its deepest traps must lie around 0.86 to 0.9eV. An alternative explanation is that at short times the

electric field strength due to the space charge and its image on the neighbouring electrode is large enough to accelerate the de-trapping process. With the removal of space charge the field will reduce and at some stage its influence upon the de-trapping process becomes negligible and the space charge decay is effectively determined by the trap depths, as in equation (3). This possibility is explored in sub-section 4.2. Finally there is the possibility that the space charge decay does not involve charge de-trapping at all, but is determined by Schottky injection (as in [4,6]) neutralising the existing space charge. This possibility is evaluated in sub-section 4.3.

4.2 Influence of Space Charge Field on De-Trapping

Usually it is assumed (see [6] for example) that in the presence of an electric field the promotion of charge from a trap that is neutral when empty is assisted by a reduction of the energy barrier in the field direction, i.e., the de-trapping probability changes as shown below,

$$P_{de-trap}(E=0) \propto \exp(-\Delta/kT) \quad \rightarrow \quad P_{de-trap}(E) \propto \exp(-[\Delta-deE]/kT) \tag{7}$$

Here d is the distance from the centre of the trap to the peak of the barrier. In the situation under discussion there is no applied field, however there is a field due to the space charge itself, which can therefore be expected to have an influence upon its own de-trapping rate. The transport of charge to an extracting electrode or a region where neutralisation can take place should thus depend upon the time dependent space charge density. The derivation of an expression for the effective charge mobility during space charge decay that was presented in [10, 11] attempted to take account of this effect in a way that would be generally applicable. However, the existence of a spatial distribution in space charge that may alter during the decay process makes it impossible to obtain a solution without the use of approximations, though their choice may be simplified when only the charge density and not the distribution alters [20]. In the measurements presented here the space charge resides in peaks near to the electrodes. The resulting electric field will be large between the space charge and the electrodes and small in the bulk between the two space charge peaks. Consequently most of the space charge will be de-trapped and move to the neighbouring electrode where it is extracted or neutralised, rather than transit the sample to recombine with charges of opposite polarity.

The electric field that influences charge de-trapping and hence the space charge decay will be that between the space charge and its neighbouring electrode. The measured space charge resides in a single peak close to the electrode and its actual distribution will be narrower than implied by the measured signal because of limitations on the spatial resolution of the signal caused by the finite width of the probe pulse and the instrument response. We have therefore approximated it as a plane of charge near to the electrode, and hence the space charge field will be uniform in the region between the space charge and the electrode with a magnitude proportional to the charge density of the peak. With these assumptions it is possible to derive an expression for the time dependence during decay of the space charge density, $\rho(t)$, in the peak considered (see Appendix 2),

$$1 - \exp(-D\rho(t)/kT) = NDe[E_1(\nu\exp(-\Delta_{max}/kT)t) - E_1(\nu\exp(-\Delta_{min}/kT)t)] \tag{8}$$

Here D is the product of the proportionality constant between electric field and $\rho(t)$, the charge on an electron, and *d*. It is therefore a material dependent constant. $E_1(..)$ is the exponential integral defined in Appendix 2. $Nd\Delta$ is the number of traps per cubic metre with trap depths between Δ and $\Delta + d\Delta$, and is assumed to be a material dependent constant. When $D \rho(t)/kT \ll 1$ equation (8) has the same form as that given in the set of equations (2) to (4), i.e. when $\rho(t)$ is small enough the barrier reduction due to the space charge field becomes negligible compared to the trap depths and space charge decay is determined by the depths of the filled traps as in section 4.1. It is therefore expected that the effect of the space charge field will only be appreciable at short times where $\rho(t)$ can be expected to be large. However the application of equation (8) to the short time experimental data is not easy so we have derived a more approximate expression for use with our data. In this case we assume that at any given time charge is only released from the shallowest filled traps. Since,

$$\rho(t) = Ne[\Delta_{max} - \Delta_{min}(t)] \tag{9}$$

where $\Delta_{min}(t)$ is the highest filled trap depth at time t, we can describe the decay of the space charge through the time dependence of $\Delta_{min}(t)$, see Appendix 2. The resulting expression applicable to the short time region where equations (2) to (4) do not fit our data is given by,

$$\exp(-G\rho(t))/G\rho(t) = A + kt \tag{10}$$

with

$$G = [1 + NeD]/(NekT) \tag{11}$$
$$A = \exp(-G\rho(0))/G\rho(0) \tag{12}$$
$$k = \nu\exp(-\Delta_{max}/kT) \tag{13}$$

When $kt > A$, equation (10) reduces essentially to the form of equation (3), as is predicted from the exact equation (8). However the time for the onset of this behaviour is dependent not just upon Δ_{min} but also upon D and N.

Equation (10) can be solved numerically for $\rho(t)$ at time t for given values of G, $\rho(0)$, and *k*. Figure 5 shows the best fit that can be achieved for the measurements at T = 33°C. A slightly improved fit is obtained at short times where the data deviated from the sigmoidal form of equations (2) to (4). Since equation (10) reduces to the form of equation (3) at long times the fit at t >10^3s is as good as before. The fit to the data shown in figure 5 suggests that the space charge generated electric field may influences charge de-trapping but only at short times when the space charge density is largest and the electric field reduction of the barrier is significant compared to Δ_{min}. In this case there would be some significant de-trapping prior to the time at which $\rho(t)$ starts to be proportional to log (t). As the charge is progressively removed the field decreases and its effect becomes negligible compared to the de-trapping activation energy. Consequently the description given in equations (2) to (4) in which the electric field is neglected becomes a good approximation over much of the observation window. This can be seen from the value of 1.125eV estimated for Δ_{max} from the fitted value of *k* (2×10^{-6} s^{-1}), which is close to the estimate given in Table 1 made from equations (2) to (4). Only where the observed space charge has a high density would we expect the space charge field to have a substantial effect upon the observed decay.

4.3 Neutralisation by Schottky Injection

It was shown in [5, 7] that on removal of the applied voltage space charge peaks near to an electrode were neutralised by Schottky injection from the electrode when the electrode field was sufficiently high, although this was not maintained at low fields [7]. It is difficult to determine whether or not such injection is taking place in the absence of measurements of the external current simultaneous with those of the space charge. However, here we take advantage of our assumption that the electrode field is proportional to the space charge to derive an expression for the time dependence of the decay of the space charge field through neutralisation of the space charge by Schottky injection from the electrode, see Appendix 3. This has the form,

$$\exp\{-B'[E_e(t)]^{1/2}\}[1 + B'[E_e(t)]^{1/2}] = [(B')^2/2]F(t) = [(B')^2/2]\{F(0) + J't\} \qquad (14)$$

where,

$$F(0) = [2/(B')^2]\exp\{-B'[E_e(0)]^{1/2}\}[1 + B'[E_e(0)]^{1/2}] \qquad (15)$$
$$B' = (e^3/4\pi\varepsilon_o\varepsilon_r)^{1/2}(1/kT) \qquad (16)$$

and J' is given by,

$$J' = (J_o)'\exp\{-\phi/kT\} \qquad (17)$$

Here $(J_o)'$ is the pre-exponential current density of the Schottky injection current multiplied by a proportionality constant that relates the electrode field to the integrated charge per unit area in the space charge peak, see Appendix 3.

These equations imply that a plot of the LHS of equation (14) (i.e. $[(B')^2/2]F(t) = \exp\{-B'[E_e(t)]^{1/2}\}[1 + B'[E_e(t)]^{1/2}]$) as a function of time t should yield a straight line if Schottky injection is the dominating process of the field (space charge) decay. The electrode field, $E_e(t)$ can be estimated from the measured space charge density, and B' evaluated using the known relative permittivity (ε_r =3.8) of the epoxy. The results for T=20 °C are plotted in figure 6a, and for 33 °C in figure 6b. These plots show a continuing curvature and very little indication of a linear behaviour for F(t) except perhaps at the longer decay times where the value of E_e becomes small. In this region we would expect the injection current, equation (1) to become effectively independent of E_e, and the time dependence of $\rho(t)$ to take the form,

$$\rho(t) = \rho' - HJ't \qquad (18)$$

with H and ρ' constants independent of time. Since $E_e(t) \propto \rho(t)$, equation (18) implies that $E_e(t)$ should also be linearly decreasing with time at long times. This can be shown by taking the limit $B'[E_e(t)]^{1/2} < 1$ in equation (14), which gives,

$$\exp\{-B'[E_e(t)]^{1/2}\}[1 + B'[E_e(t)]^{1/2}] \rightarrow 1 - (B')^2 E_e(t) = [(B')^2/2]\{F(0) + J't\} \qquad (19)$$

Thus the near linear regions at long times in figure 6 can be associated with a time dependence of $\rho(t)$ in the form of equation (18), and hence with a field independent current leading to charge neutralisation. The only region of time where the data shows

some agreement with the predictions of neutralisation by charge injection is therefore that for which the space charge field has become negligible, and injection is governed solely by thermal activation. An estimation of the activation energy involved can be obtained by determining the values of J' from the gradients of the linear regions of the two plots and using equation (17). In this way we find $\phi = 0.97eV$, which lies in the same range as Δ_{min} to Δ_{max} given in Table 1. It is clear that the thermally activated process that gives rise to the long time behaviour has essentially the same activation energy as that involved in the de-trapping model considered in sub-sections 4.1 and 4.2. In view of the fits obtained for a distribution of trap energies (see figure 4) it is likely that curvature that can still be observed in figure 7 at long times is a consequence of restricting the analysis to the unique activation energy of the Schottky expression given in equation (1). There is thus no evidence for the existence of Schottky injection at short times where the space charge field could be expected to have an effect. Instead the data implies that space charge decay is governed by a field-independent injection or extraction current requiring thermal activation of around 1 eV.

5. <u>DISCUSSION</u>

A single general mechanism for the decay of space in dielectric materials cannot be expected to hold because there are many processes that may take place. As a rule of thumb, we would expect charge neutralisation by transit of the sample to result in an extension of the space charge further into the bulk region unless there is independent evidence for a high conductivity in the body of the material such as may be found in some heterogeneous materials. When there are isolated space charge peaks that essentially retain their shape during decay, neutralisation can be expected to occur via extraction or injection currents involving a neighbouring electrode. This is the case here. It is important to note that the time dependence of the space charge decay is governed by the slowest of the processes that take place. For example, trapped space charge must be de-trapped and then travel to the electrode for neutralisation or extraction. If extraction at the electrode is an ohmic process it will essentially be instantaneous, however if extraction is not ohmic it will have a time scale determined by the mechanism controlling the current across the electrode-dielectric interface. The time dependence of space charge decay will be determined by which of the three possible processes is the slowest, i.e. the rate determining step.

In section 4 we have evaluated the space charge decay in terms of two alternative mechanisms: release of charge for extraction by a single de-trapping process (with and without space-charge field assistance), and neutralisation by Schottky injection. Both processes have been shown to occur in previous work [5, 7, 9]. The essence of the single de-trapping process is that during transit to the electrode the charge has to be de-trapped only once from a trap level at the top of the filled range. This therefore becomes the rate determining step as intermediate steps involving de-trapping from shallower traps take much less time. Only at times less than 10^2s is there any evidence for the influence of the space charge field, with the data providing a reasonable fit to the field-assisted de-trapping model (see figure 5) but not to an explanation based on Schottky injection (see figure 6). Even in this time range the involvement of the space charge field is not conclusively demonstrated since the data could be equally well described by field-independent charge de-trapping from a shallower set of traps.

Our analysis has shown that over most of the measurement time window the decay of the space charge is governed by a field-independent thermally activated process. Two possibilities exist for the origin of this process: a) a thermal injection/extraction current at the electrode, and b) space charge de-trapping. Figures 6a & 6b show that the linear behaviour predicted from thermal injection with unique activation energy, equation (19), is only poorly reproduced. In view of the good fit in the same time range to charge de-trapping from traps that are distributed in trap depth (see figure 4), it seems likely that the thermal activated charge decay process must involve such a distribution whether or not it relates to extraction or neutralising injection. On the face of it extraction or injection are equally likely mechanisms given a distribution in activation energies. However, it should be noted that if injection is the operative mechanism the space charge observed must be unable to move over the time of the experiment, while awaiting neutralisation. This would imply either that the space charge resides in traps with a depth greater than 1.2 eV or that it was due to ionic centres forming part of the epoxy matrix.

We have examined a situation in which the decay process involved currents between the space charge a neighbouring electrode, where the transit to the electrode can be assumed to be fast as in [9] once the charge is de-trapped. Since the de-trapping controls the decay current it is possible to interpret the space charge decay in terms of an effective mobility [11, 20]. It must be understood though, that in our case this mobility would be that of the space charge in the region where it is trapped. If the space charge has to move through regions of different space charge density or space charge polarity, as for example during a transit of the sample, it will trap into the deepest available traps. These will not be the deepest unfilled traps of the space charge region as in equations (2) to (4). In this case the mobility would probably not change very much over time.

Our analysis also shows that a uniform distribution of trap energies between $\sim 0.94\text{eV}$ and 1.15eV describes the data very well. Such a top-hat distribution is most probably an idealisation of the actual physical situation but the precision of our data is unlikely to be able to detect minor variations relating to the difference between such a distribution and a Gaussian (normal) distribution. However, it should be noted that in [9] a larger amount of data from a different epoxy similarly reveals a top-hat distribution. There it was shown that $\Delta_{max} = 0.94\text{eV}$ at both T=25 °C and T=35 °C. However Δ_{min} was shown to reduce as the applied voltage increased and the amount of charge injected increased. For this reason it was suggested that Δ_{max} relates to the deepest trap available in the timescale of voltage application, and that the traps are filled up to a trap depth of Δ_{min}. The results presented here are consistent with that view with a value of Δ_{max} that remains essentially unchanged with temperature whereas Δ_{min} shows some minor variations that may be due to small differences in the space charge density. The limited data from $t < 10^2\text{s}$ also indicate that there may be shallower traps with depths less than 0.9eV. Given the time window of our experiments we would not be able to detect the decay of charge in traps of less than about 0.82eV at these temperatures and hence are not able to identify their existence for certain. TSC experiments [8] however, typically reveal more than one peak in the trap distribution, and hence it would not be unexpected for more than one trap distribution to be present in our material. The length of time over which we measured the decay shows however, that any charge trapped below 1.15 eV is too small to be detectable by our equipment even if it exists, and therefore it is reasonable to argue

that our maximum trap depth represents the deepest traps available to the injected charge during the experiment.

The samples used in [9] require wires to be moulded inside them that act as the high voltage terminal during voltage application and it could be argued that the traps were introduced during their manufacture. The existence of a top-hat distribution of traps in the epoxy resin investigated here in parallel plate geometry show that this is not the case. However both epoxy resins investigated were in their glass state and this raises the question as to whether or not these traps relate to frozen-in states of the material or originate with the hetero-atoms that are part of the chemical composition of epoxy resins. If the former is the case we would expect to find a different picture above the glass transition temperature, whereas the results should have essentially the same form in the latter situation. This is particularly pertinent because the polyethylene materials, which are in a rubbery state, showed evidence for a different mechanism, that of neutralisation by Schottky injection [5, 7]. In one case [5] it seems that the space charge was associated with molecular ions and neutralisation by charge injection would be the only viable mechanism for space charge decay if it is assumed that during the voltage application time the donated carriers had transited to the counter electrode and a substantial portion extracted. In the other case the nature of the charges is not clear, but semiconductor electrodes were used and hence it is possible that they were also molecular ions originating either from the semiconductor or from molecular additives or residues within the polymer. Accordingly we performed a similar experiment (+2kV for 42h followed by voltage removal) on the resin at a temperature of 50 °C where it above the glass transition. The results are shown in figure 7. In this case there is no detectable decay of the space charge peak over a period of 1s to 27s following the removal of the voltage. We can use equation (6) to estimate that the shallowest traps in which the observed space charge resides at this temperature lies deeper than 0.914eV. This estimate is consistent with the values given in Table 1, but the amalgamation of the space charge peak with the electrode peak at 200s (see section 3.2) makes it difficult to make any estimate of the trap depth energy range and distribution. It was noted however that this peak remained unchanged for several hours [21] so it is likely that the trap depth range is similar to that found below the glass transition, and hence that the traps are associated with the hetero-atoms of the chemical structure.

The conversion of the signal to a single peak near the electrode tends to occur at progressive shorter times as the temperature increases, Table 2. This is consistent with explanation given in section 3.2. As the temperature increases the space charge decay occurs faster and hence the electrode field reduces to a level at which the first order contribution to the signal drops below that of the second order contribution at an earlier time.

6. CONCLUSIONS

Given sufficient stressing time space charge can be injected into epoxy resins at fields as low as 7.14kV/mm. This is trapped near to the injecting electrode forming homo-charge peaks. Some of this charge will remain in the sample beyond 100 hours after voltage removal. At such long decay times the space charge peak may become obscured by the probe-pulse generated signal at the electrode-dielectric interface.

There is no substantive evidence for an involvement of the space charge field in the decay process.

The space charge decay is governed by de-trapping from charge traps whose depths range from about 0.94eV to 1.15eV with an essentially uniform distribution.

The time over which space charge can be retained in the epoxy resin depends upon the depth of the deepest traps occupied and the temperature.

The same decay process is operative both above and below the glass transition, though the de-trapping rate increases as the temperature increases.

REFERENCES

[1]. Y.Zhang, J.Lewiner, C.Alquie, and N.Hampton, "Evidence of strong correlation between space-charge buildup and breakdown in cable insulation", IEEE Trans. DEI, vol. 3, pp778-783, 1996
[2]. M.A. Brown, G. Chen, A.E. Davies, L.A. Dissado and P.A. Norman, "Space charge characterisation in aged LDPE amalgamated insulation regions from underwater telecommunication systems", IEEE Trans. Diel. & EI, **7**, pp.346-352, 2000
[3]. R.Bartnikas, "Performance characteristics of dielectrics in the presence of space charge", IEEE Trans.DEI, vol.4, pp544-557, 1997;
[4].Y.F.F.Ho, G. Chen, A.E. Davies, S.G. Swingler, S.J.Sutton, R.N.Hampton, and S.Hobdell, "Measurement of space charge in XLPE insulation under 50Hz AC electric stresses using the LIPP method", IEEE Trans. Diel. & EI, **9**, pp.362-370, 2002
[5] Y.Suzuoki, H.Muto, T.Mizutani, and M.Ieda, "Effects of space charge on electrical conduction in high- density polyethylene", J..Phys..D:Appl.Phys. vol.18, 2293-2302, 1985
[6] L.A.Dissado and J.C.Fothergill, *Electrical Degradation and Breakdown in Polymers* Pub. By P.Peregrinus for IEE, London, U.K (ISBN 0 86341 196 7) 1992.
[7] P.Morin, J.Lewiner, C.Alquie, and T.Ditchi, "Study of space charge dynamics in solid dielectrics by simultaneous measurement of external current and space charge distributions", in *Space Charge in Solid Dielectrics* Eds. L.A.Dissado & J.C.Fothergill, Pub. The Dielectrics Society, Leicester U.K. (ISBN 0 9533538 0X), 43-57, 1998
[8] M.Ieda, T.Mizutani, and S.Ikeda, "Electrical conduction and chemical structure of insulating polymers", IEEE Trans. EI, vol21, pp301-306, 1986
[9] L.A.Dissado, O.Paris, T.Ditchi, C.Alquie, J.Lewiner, "Space charge injection and extraction in high divergent fields", Ann.Rep. CEIDP (IEEE Pub. 99CH36319), pp23-26, 1999
[10] G.C.Montanari,G.Mazzanti, F.Palmieri, G.Perego, S.Serra, "Space-charge trapping and conduction in LDPE,HDPE, and XLPE", J.Phys.D:Applied Physics, Vol.34, pp2902-2911, 2001
[11]. G.Mazzanti, G.C.Montanari, J.M.Alison, "A space-charge based method for the estimation of apparent mobility and trap depth as markers for insulation degradation.Theoretical basis and experimental validation" IEEE Tans. DEI, vol. 10, pp187-197, 2003.
[12] T.Takada, "Acoustic and Optical Methods for Measuring Electric Charge Distributions in Dielectrics", IEEE Tran. DEI, vol 6, pp519-547, 1999

[13] V.Griseri, L.A. Dissado, J.C.Fothergill, G. Teyssedre, C.Laurent, "Electroluminescence Excitation Mechanism in an Epoxy Resin under Divergent and Uniform Field", IEEE Trans Diel & E.I., Vol.9, pp150-160, 2002.

[14] S.Hole, T.Ditch, and J.Lewiner, " Non-destructive Methods for Space Charge Distribution Measurements: What are the differences", IEEE Trans. DEI, vol 10, pp670-677, 2003

[15] J.Lewiner, S.Hole, and T.Ditchi, "Pressure Wave Propagation Methods: a rich history and a Bright Future", IEEE Trans. DEI, vol 12, pp114-126, 2005

[16] M.P.Cals, J.Marque, and C.Alquie, "Application of the pressure wave propagation method to the study of interfacial effects in irradiated polymer films", J.Appl.Phys., vol.72, pp1940-1951, 1992

[17] S.Hole, V.Griseri, L.A.Dissado and J.C.Fothergill, " Improvement of PEA signal analysis using simulations for complex geometry samples", J.Phys.D:Appl.Phys., vol. 35, pp19-34, 2002

[18] J.M.Alison, "The pulsed electro-acoustic method for the measurement of the dynamic space charge profile within insulators", in Space Charge in Solid Dielectrics, (pub. The Dielectrics Society, Leicester, 1998, ISBN 0 9533538), Eds.J.C.Fothergill and L.A.Dissado, pp93-121, 1998

[19] P.K.Watson, "The transport and trapping of electrons in polymers", IEEE Trans. DEI, vol.2, pp915-924, 1995

[20] J.M.Alison, G.Mazzanti, G.C.Montanari, and F.Palmieri, "Mobility estimation in polymeric insulation through space charge profiles derived by PEA measurements", Ann. Rep. CEIDP (IEEE pub. 02CH37372), pp25-39, 2002

[21] V.Griseri, PhD Thesis "The Effects of high Electric Fields on an Epoxy Resin", The University of Leicester, U.K, 2000

[22] M. Abramowitz and I.A.Stegun, *Handbook of Mathematical Functions* (Dover Press, New York, 1965)

Table 1. Values of the minimum (Δ_{min}) and maximum (Δ_{max}) trap depths estimated from equations 3 to 5, and used to produce the fitted curves in figure 5.

Temperature (K)	Δ_{min} (eV)	Δ_{max} (eV)
306	0.97	1.13
298	0.98	1.14
293	0.94	1.1

Table 2. Time at which only a single peak is observed near the lower electrode.

Temperature (K)	Estimated Time of Amalgamation
293	t > 22 hours
298	48 hours > t > 4 hours
306	18 hours > t > 3.5 hours
323	200s > t > 27 s

<u>TABLE CAPTIONS</u>

<u>Table 1.</u> Values of the minimum (Δ_{min}) and maximum (Δ_{max}) trap depths estimated from equations 3 to 5, and used to produce the fitted curves in figure 5.

<u>Table 2.</u> Time at which only a single peak is observed near the lower electrode.

<u>FIGURE CAPTIONS</u>

<u>Figure 1</u>. Space charge measured at various times after removal of the voltage (plus 5min, cross 4h, black diamond 48h, white diamond 68h); T = 25 °C. The anode and cathode labels refer to the polarity of the electrodes during the application of the voltage. The label 'positive homomocharge' refers to the nature of the charge during voltage application. The charges seen on the electrodes in the figure are the combination of the image charges induced by the positive space charge peak and the signal produced by the probe pulse itself. The x-axis relates to the distance along an axis perpendicular to the electrodes, and the sample thickness is noted.

<u>Figure 2</u>. (a) Magnitude of the electrode charge plotted as a function of the homo-charge peak magnitude (T=20 °C) during the period of decay when both peaks can be observed. The linear dependence is indicated by the dashed line. (b) PEA signal measured before the application of a voltage. This plot is obtained in the same way as those in Figure 3.

<u>Figure 3</u>. Sample and probe polarity reversal tests after 114 h depolarisation at T = 33 °C. (a) Example of procedure for de-noising the data (i) smoothing by finding a 19-point running average, (ii) finding the best fit to the DC baseline drift, (iii) removing the baseline drift. (b) Set of traces, 1 :- +400V pulse sample in original orientation, 2:- +400V pulse sample reversed, 3:- -400V pulse sample reversed, 4:- -400V pulse sample in original orientation, 5:- +400V pulse sample in original orientation

<u>Figure 4</u>. The space charge density $\rho(t)$ of the peak next to the lower electrode plotted as function of log(t) with the time in seconds.
a) data from T = 25 °C (Figure 1); fitted line uses equation (25) with Δ_{min} and Δ_{max} given in Table 1, and N = 1.24x10^{39} m^{-3} J^{-1}
b) uncalibrated PEA signal from 33°C; fitted line from equation (25) with Δ_{min} and Δ_{max} given in Table 1, and N = 8.1x10^{37} (arb. units)
c) uncalibrated PEA signal ($\propto \rho(t)$) from T = 20°C; fitted line from equation (25) with Δ_{min} and Δ_{max} given in Table 1, and N = 6.65x10^{37} (arb. units)

<u>Figure 5</u>. A plot of log (S(t) at T= 33°C as a function of log(t) (time in seconds), where S(t) ($\propto \rho(t)$) is the uncalibrated PEA signal. The diamonds are the data points and the line is the best fit to equation (10) with ***k***= 2 10^{-6} s^{-1} (equivalent to Δ_{max} = 1.125 eV) and G = 1.5 10^{4} arb. units.

Figure 6. Plot of $\exp\{-B'[E_e(t)]^{1/2}\}[1 + B'[E_e(t)]^{1/2}]$ as a function of time t (seconds), with $z = E_e(t)]^{1/2}$: a) data from T=20 °C, b) data from T=33 °C. A linear relationship would be expected if Schottky injection is responsible for the charge decay.

Figure 7. Space charge measurements at T =50 °C, E =6.7 kV/mm (applied voltage = 2kV). Top: Space charge distribution under voltage and immediately after voltage removal. Bottom: Space charge decay, dashed line t=1s, triangle t=11s, dotted line t=27s, squares t=200s.

APPENDIX 1.

The derivation of equation (3) starts with the assumption that the promotion of charges from a given trap depth is independent of promotion from other traps. The time dependence of the occupancy, N(t), of the traps at a trap depth Δ then becomes,

$$N(t) = N\exp\{-\nu t\exp(-\Delta/kT)\} \tag{20}$$

and,

$$d\{N(t)\}/dt = -N(t)\,\nu\exp(-\Delta/kT) \tag{21}$$

where $N\,d\Delta$ is the number of traps per cubic metre with an energy between Δ and $\Delta+d\Delta$ at t = 0. The total rate of removal of charges from traps with depths between Δ_{max} and Δ_{min} is therefore given by,

$$d\{\rho(t)\}/dt = -e\,\nu N \int_{\Delta_{min}}^{\Delta_{max}} e^{-\Delta/kT}\exp\{-\nu t\,e^{-\Delta/kT}\}d\Delta \tag{22}$$

The integral over Δ can be solved using the substitution $Y=\nu\exp\{-\Delta/kT\}$, which gives,

$$d\{\rho(t)\}/dt = (eNkT/t)[\exp\{-\nu t Y_{max}\} - \exp\{-\nu t Y_{min}\}] \tag{23}$$

where,

$$Y_{max} = \exp\{-\Delta_{min}/kT\} \quad \text{and} \quad Y_{min} = \exp\{-\Delta_{max}/kT\} \tag{24}$$

Integrating equation (23) between time t and infinity gives the residual charge density,

$$\rho(t) = eNkT[E_1(\nu t Y_{min}) - E_1(\nu t Y_{max})] \tag{25}$$

where $E_1(x)$ is the exponential integral [19] defined by,

$$E_1(x) = \int_x^\infty \frac{e^{-t}}{t}\,dt \tag{26}$$

Standard expansions [22] for $E_1(x)$

$$E_1(x) = -\ln(x) - 0.57721 \qquad\qquad x < 1 \tag{27}$$

$$E_1(x) \sim e^{-x}/x \qquad\qquad x > 1 \tag{28}$$

yield the set of equations (2) to (4).

APPENDIX 2.

The inclusion of the space charge field into an expression for space charge decay starts with the field-dependent de-trapping probability,

$$P_{de-trap}(E) \propto \exp(-[\Delta - deE]/kT) \tag{29}$$

The electric field E is that acting between the space charge peak and the electrode produced by the space charge itself. It can therefore be assumed to be proportional to the space charge density, ρ, and at a given time t,

$$D\rho(t) = deE(t) \tag{30}$$

where D is a time and space charge independent constant containing the proportionality factor between ρ and E. The field dependent term in equation (29) is independent of the trap depth, Δ, and hence equation (23) becomes,

$$d\{\rho(t)\}/dt = (eNkT/t)\exp\{D\rho(t)/kT\}[\exp\{-vtY_{max}\} - \exp\{-vtY_{min}\}] \tag{31}$$

Equation (31) can be integrated between time t and infinity as before, to yield equation (8),

$$1 - \exp(-D\rho(t)/kT) = NDe[E_1(v\exp(-\Delta_{max}/kT)t) - E_1(v\exp(-\Delta_{min}/kT)t)] \tag{8}$$

The value of D is not known *a-priori* and since equation (8) is cumbersome to work with in the region where $D\rho(t)/kT > 1$, we have carried through a simplified derivation. Instead of assuming that promotion from traps of all depths occurred simultaneously but independently, we assume that during the space charge decay the traps are emptied in sequence from the shallowest to the deepest. We can now write $\rho(t)$ as in equation (9),

$$\rho(t) = Ne[\Delta_{max} - \Delta_{min}(t)] \tag{9}$$

and,

$$d\{\rho(t)\}/dt = -v\exp\{-\Delta_{min}(t)/kT\}\exp\{D\rho(t)/kT\}\rho(t) \tag{32}$$

Substituting for $\Delta_{min}(t)$ from equation (9) gives,

$$d\{\rho(t)\}/dt = -k\exp\{\rho(t)/NekT\}\exp\{D\rho(t)/kT\}\rho(t) \tag{33}$$

with,

$$k = v\exp\{-\Delta_{max}/kT\} \tag{34}$$

Integration of equation (32) gives,

$$E_1(G\rho(0)) - E_1(G\rho(t)) = -kt \tag{35}$$

where $E_1(x)$ is the exponential integral as before and G is as given in equation (11),

$$G = [1 + \text{N}e\text{D}]/ \text{ N}e\text{kT} \tag{11}$$

Use of the large x expansion for $E_1(x)$, equation (28), allows us to obtain equation (10) for $\rho(t)$ that is valid in the short time region where $\rho(t)$ is largest,

$$\exp(-G\rho(t))/G\rho(t) = \text{A} + \boldsymbol{k}t \tag{10}$$

with,

$$\text{A} = \exp(-G\rho(0))/G\rho(0) \tag{12}$$

APPENDIX 3.

The rate of injection of neutralising charge by means of a Schottky injection current, equation (1) depends upon the electric field at the electrode, and is given by,

$$dQ'/dt = \text{J}_o\exp\{-\phi/kT\}\exp\{B'[E_e(t)]^{3/2}\} \tag{36}$$

where Q' is the injected charge per unit area, J_o is the Schottky current density pre-exponential factor, see equation (1), and,

$$B' = (e^3/4\pi\varepsilon_o\varepsilon_r)^{1/2}(1/kT) \tag{16}$$

The injected charge per unit area, Q', will reduce the integrated space charge in the sample. Where the space charge peak is close to the electrode and does not change its shape appreciably during its decay following voltage removal, as here, we may assume that $E_e(t)$ is proportional to the space charge density $\rho(t)$ of the peak and hence,

$$d\{E_e(t)\}/dt \propto d\{\rho(t)\}/dt \propto -dQ'/dt \tag{37}$$

Using this relationship, equation (36) becomes,

$$d\{E_e(t)\}/dt = (\text{J}_o)' \exp\{-\phi/kT\}\exp\{B'[E_e(t)]^{1/2}\} = \text{J}' \exp\{B'[E_e(t)]^{1/2}\} \tag{38}$$

where $(\text{J}_o)'$ includes the proportionality constant between Q' and E_e. The integral of equation (38) takes the form,

$$\int_{E_e(0)}^{E_e(t)} \exp\{-B'[E_e(t)]^{1/2}\}d\{E_e(t)\} = -\int_0^t J'dt = -J't \tag{39}$$

Converting the variable to $[E_e(t)]^{1/2}$ allows the Left Hand Integral to be solved via integration by parts giving,

$$[2/(B')^2]\exp\{-B'[E_e(t)]^{1/2}\}[1 + B'[E_e(t)]^{1/2}] = F(0) + J't \tag{40}$$

which can be re-arranged to give equation (14) with,

$$F(0) = [2/(B')^2]\exp\{-B'[E_e(0)]^{1/2}\}[1 + B'[E_e(0)]^{1/2}] \tag{15}$$

Figure 1

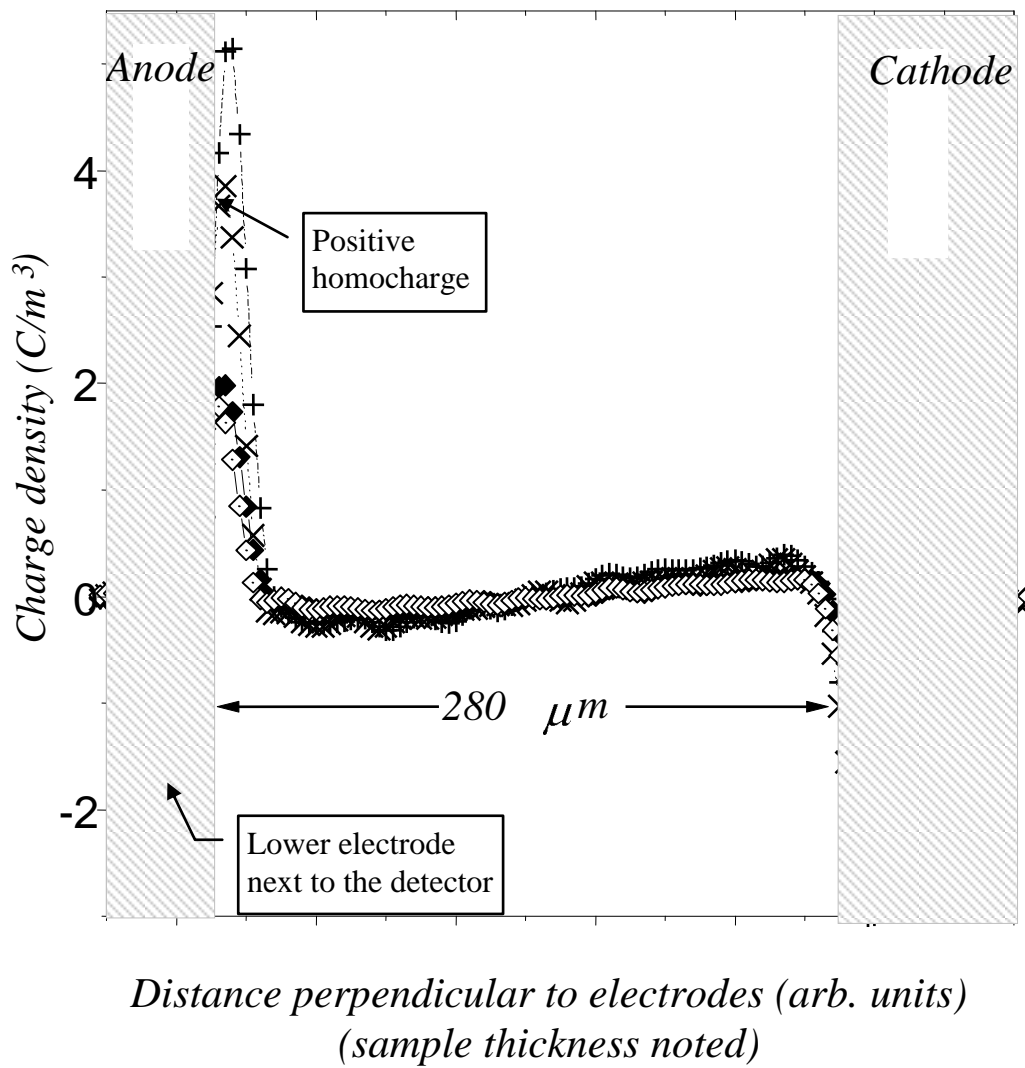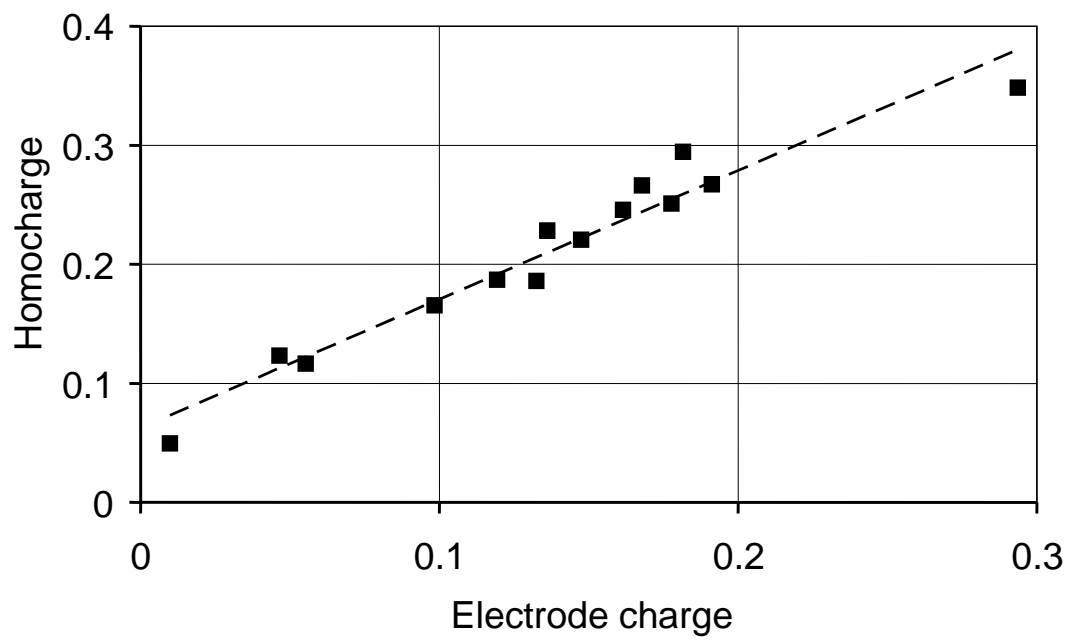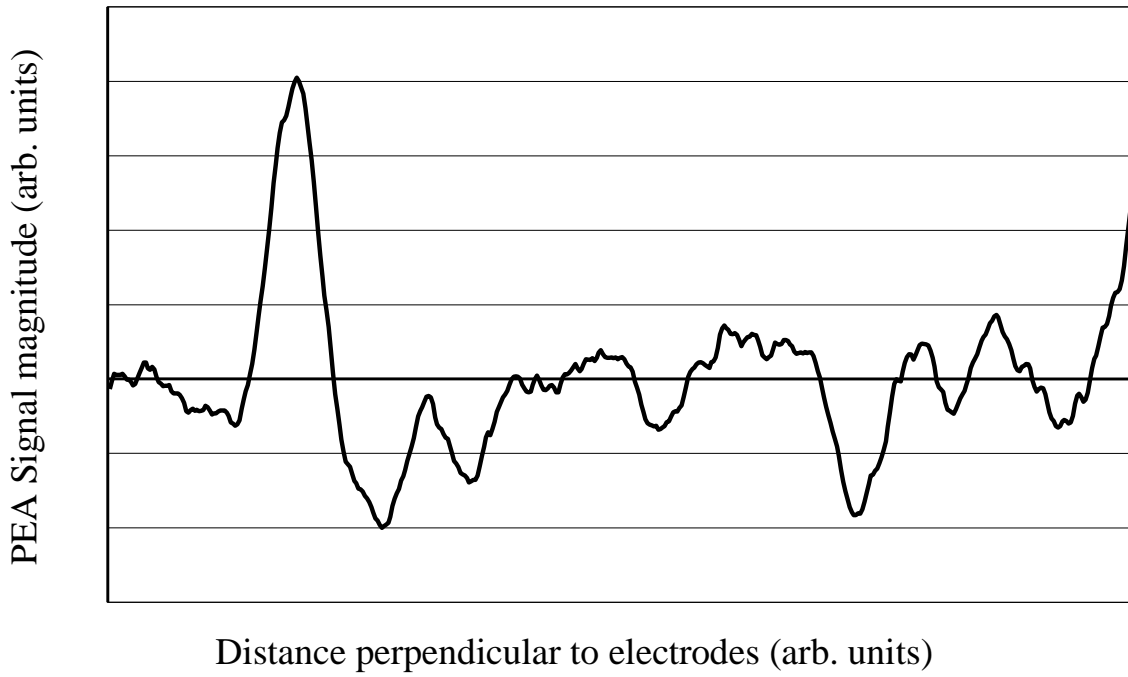
Distance perpendicular to electrodes (arb. units)
(sample thickness noted)

Figure 2(a)

Figure 2(b)

PEA Signal magnitude (arb. units)

Distance perpendicular to electrodes (arb. units)

Figure 3(a)

Distance perpendicular to electrodes (arb.units)

The figure's y-axis is labelled "Deconvoluted PEA Signal (arb. units) :- Traces displaced for clarity". The legend reads: raw data, smoothed, DC drift, drift removed.

Figure 3(b)

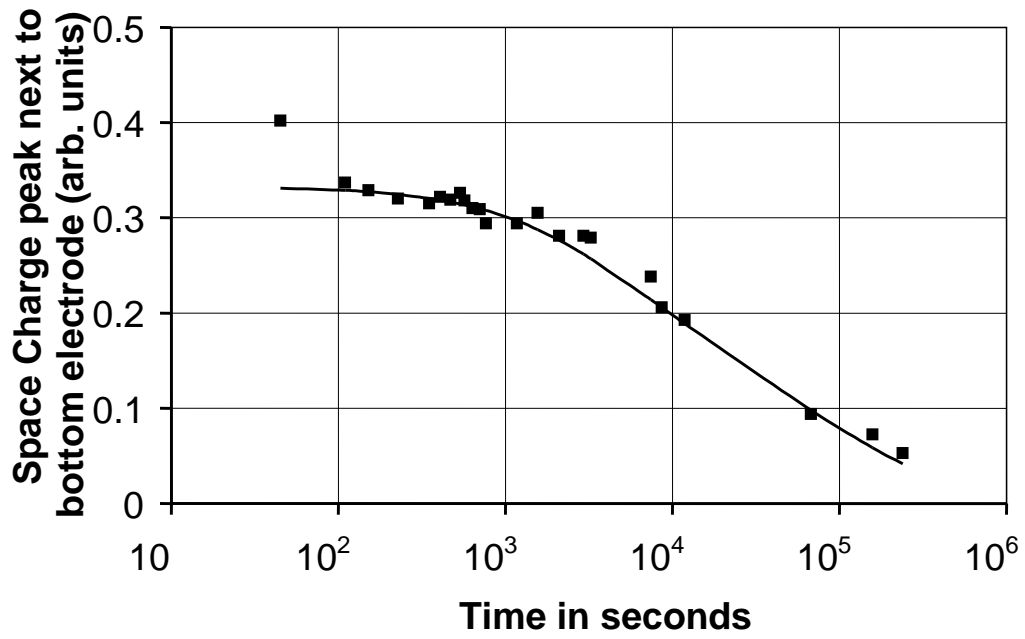Distance perpendicular to electrodes (arb.units)
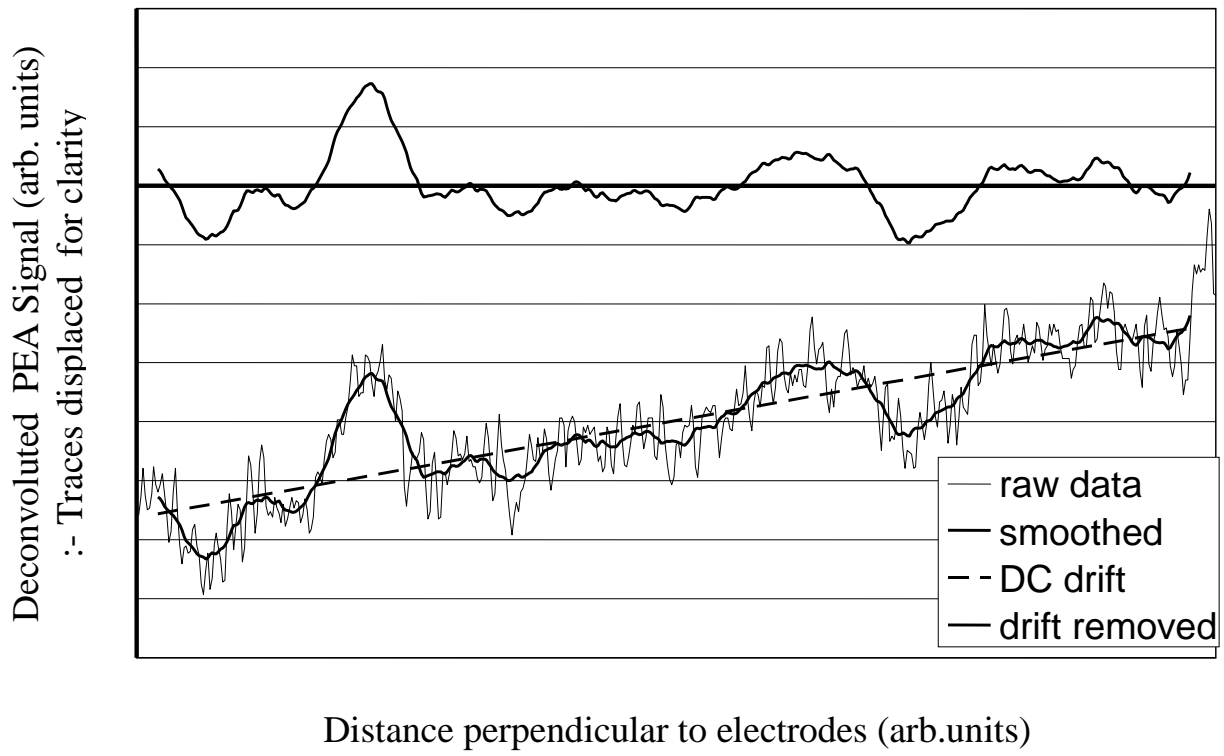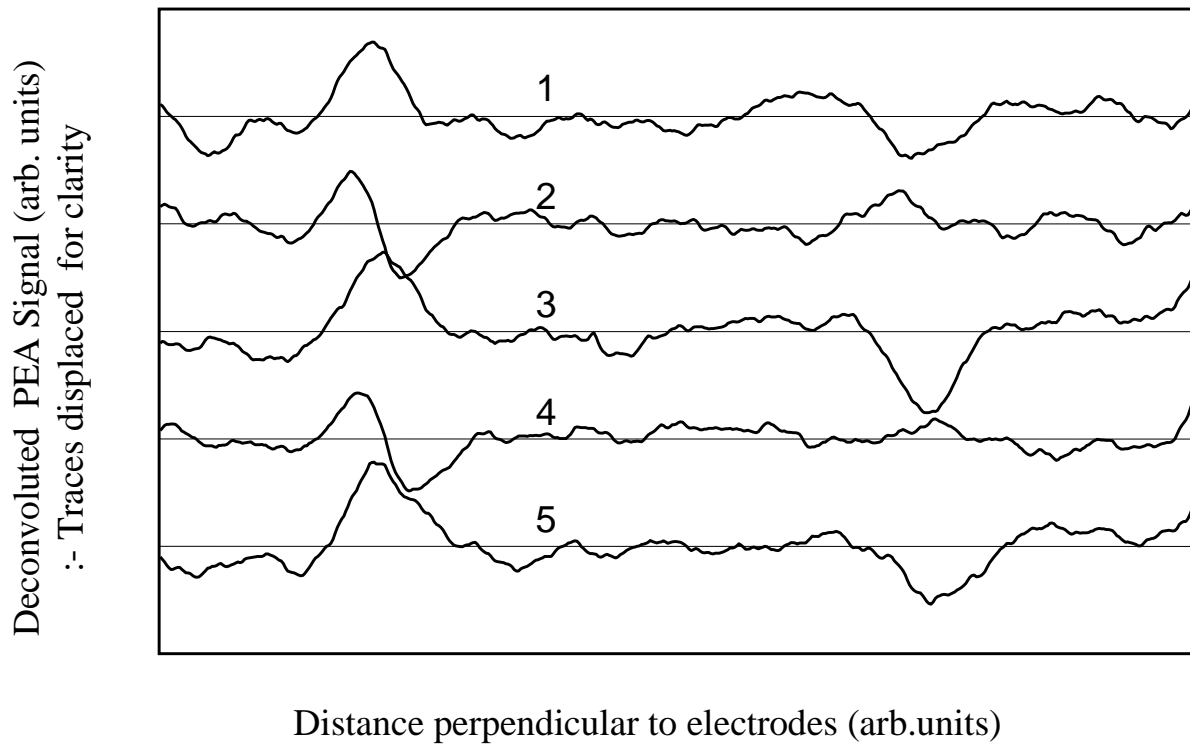
Figure 4((a)

Figure 4(b)

Figure 4(b)

Figure 4(c)

The y-axis is labeled "Space charge peak next to the bottom electrode (arb. units)" with values 0.0, 0.1, 0.2, 0.3, 0.4. The x-axis is labeled "time in s (logscale)" with values 10^1, 10^2, 10^3, 10^4, 10^5, 10^6.
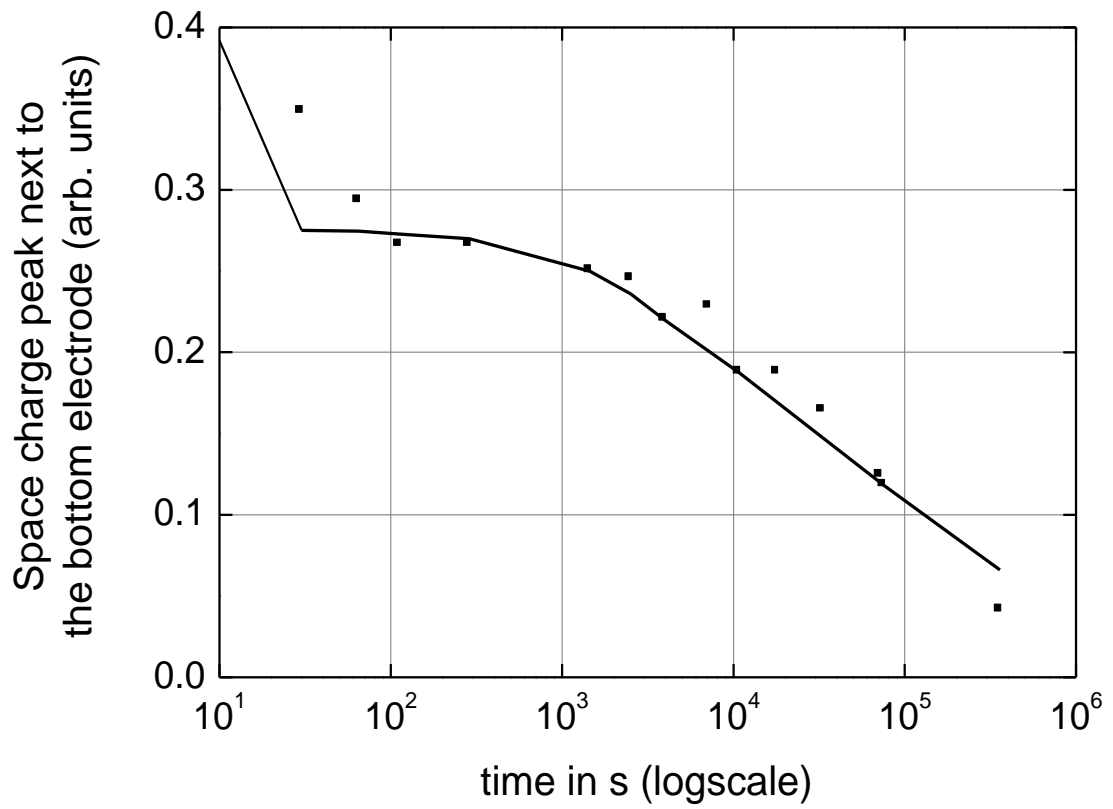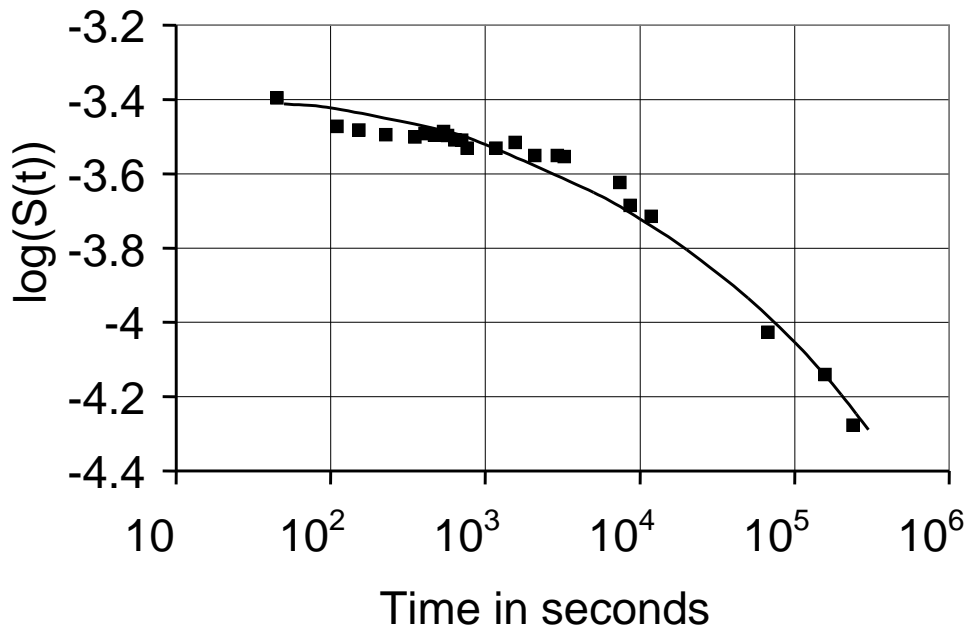
Figure 5.

Figure 6(a)

Figure 6(a)

Axis labels:
- Y-axis: $[1+Bz(t)]\exp(-Bz(t))$
- X-axis: **Time in seconds**

Figure 6(b)

Figure 7.

Distance Perpendicular to electrodes (arb.units)
(Sample thickness noted on top diagram)
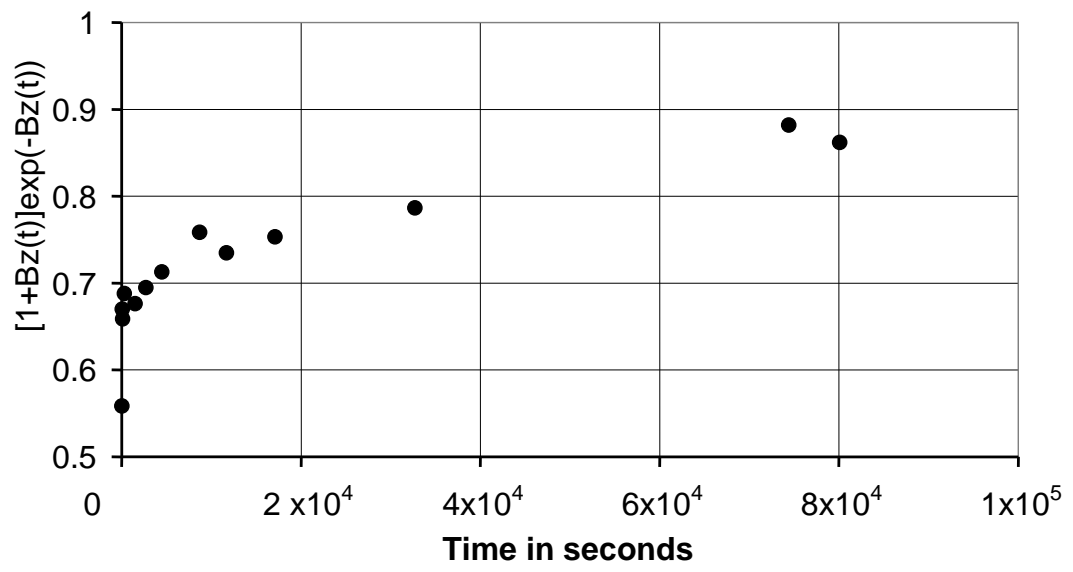
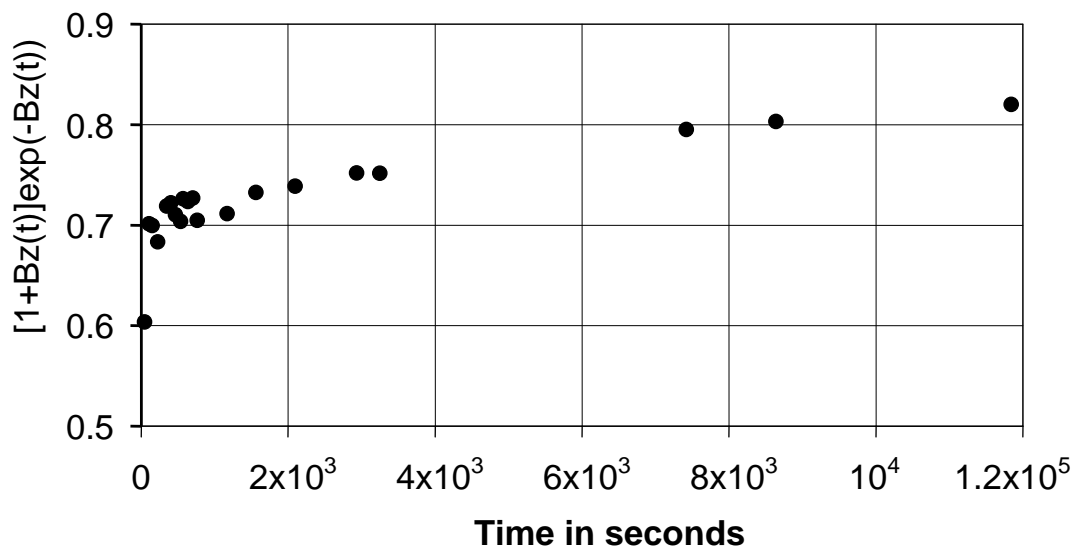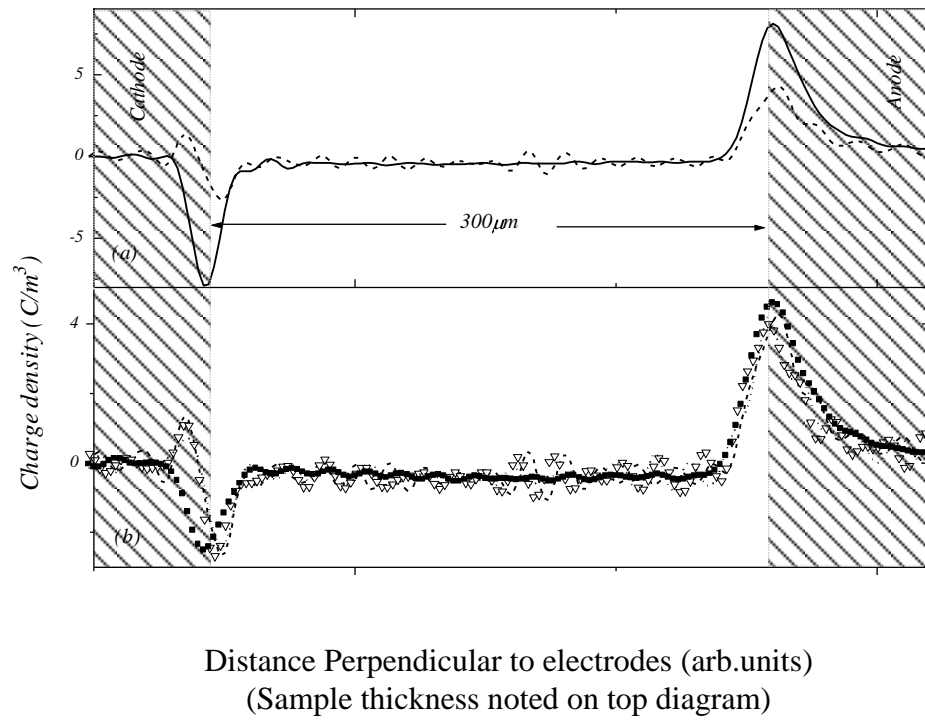## Biographies
Leonard A Dissado: (SM'96, F'06)

Born: St.Helens, Lancashire, U.K 29 August 1942

Educated: Thomas Linacre Technical School, Wigan, Lancashire, 1953-1960, gaining a State Scholarship for University Entry in 1959

Graduated from University College London with a 1st Class degree in Chemistry in 1963 and was awarded a PhD in Theoretical Chemistry in 1966 and DSc in 1990. After rotating between Australia and England twice he settled in at Chelsea College in 1977 to carry out research into dielectrics. His interest in breakdown and associated topics started with a consultancy with STL begun in 1981. Since then he has published many papers and one book, together with John Fothergill, in this area. In 1995 he moved to The University of Leicester, and was promoted to Professor in 1998. He has been a visiting Professor at The University Pierre and Marie Curie in Paris, Paul Sabatier University in Toulouse, and Nagoya University, and has given numerous invited lectures, the most recent of which was the Whitehead lecture at CEIDP 2002 in Cancun, Mexico. Currently he is an Associate Editor of IEEE Transactions DEI, co-chair of the Multifactor Aging Committee of DEIS and a member of DEIS Administrative Committee.

Virginie Griseri (non-member)

Received her M. Sc. in polymer physics from Paul Sabatier Toulouse-France University, in 1997 and received her Ph.D. degree in electrical engineering from Leicester-UK University in 2000. She spent two-years as an external CNES post-doctoral fellow at ONERA in the space studies department in Toulouse. In 2003, she joined the Electrical Engineering Laboratory at the Paul Sabatier University where she is now a Lecturer. Her current research interests include space charge and electrical ageing phenomena in polymers.

William Peasgood (non-member)

W. **Peasgood**, was born in Leicester, UK, on 30th July 1967. This author was educated at St. John the Baptist Junior School, Lancaster Boys' Secondary School and then Charles Keene College of Further Education, all in Leicester. An upper second (2:1) Joint Honours Degree in Physics with Applied Physics and Electronics was gained at Nottingham University, Nottingham, UK in 1988 and was awarded the Bill Moore Prize for outstanding contribution to final year project work. He gained a PhD in Medical Electronics at Nottingham University, Nottingham, UK in 1993 specialising in the digital extraction of the abdominal fetal electrocardiogram. The authors main field of interest is the research and design of medical equipment for diagnosis and electronic systems for rehabilitation and has a general interest in dielectric properties of materials.

He currently works as a HEALTHCARE SCIENTIST since February 2003 for the National Health Service (NHS) at the Walsgrave Hospital, Coventry, UK. Previous academic positions were held as LECTURER in Engineering at Leicester University, UK (1998-2003) and RESEARCH ASSOCIATE in Engineering at Bristol University, UK (1994-1998). Current research topics include functional electrical stimulation devices and dielectric modelling of nerve and muscle.

Dr Peasgood is an Associate member of Institute of Physics and Engineering in Medicine (IPEM) and an Associate member of the Dielectrics Society within the Institute of Physics (IOP).

Elizabeth S. Cooper (non-member)

Elizabeth Cooper was born in the UK in 1976 and gained a degree in Physics with Astrophysics from the University of Leicester in 1999. In 2002 she received a PhD, also from the University of Leicester. She worked with Professors Dissado and Fothergill in the high voltage laboratory of the engineering department at Leicester until 2004, researching the physical processes relevant to charge movement in the insulation of high voltage DC power cables. She is now a research active housewife and mother.

Kaori Fukunaga (M'96)

Kaori Fukunaga was born in Tokyo, Japan on 14 December 1963. She received the Ph.D. degree in electrical engineering from Tokyo Denki University, Tokyo, in 1993. From 1989 to 1993, she worked on high voltage cable systems at Fujikura, Ltd. She joined NICT (formerly Communications Research Laboratory) in 1995, and is a Senior Researcher of EMC Project Office. She has been involved in space charge behaviour of functional polymers, high frequency characteristics of dielectrics used in telecommunications. She is a member of the Institute of Physics, IEE of Japan, and the Japan Institute of Electronics Packaging.

John C. Fothergill (SM'95, F'04)

John Fothergill was born in Malta in 1953. He graduated from the University of Wales, Bangor, in 1975 with a Batchelor's degree in Electronics. He continued at the same institution, working with Pethig and Lewis, gaining a Master's degree in Electrical Materials and Devices in 1976 and doctorate in the Electronic Properties of Biopolymers in 1979. Following this he worked as a senior research engineer leading research in electrical power cables at STL, Harlow, UK. In 1984 he moved to the University of Leicester as a lecturer. He now has a personal chair in Engineering and is currently Pro-Vice-Chancellor.